Azhar Int J Pharm Med Sci 2022; Vol 2 (2):70-82
(Research Article)

Open Acces

Print ISSN: 2735-4598
Online ISSN: 2735-4601

Trifluoperazine-loaded leciplexes as potential nasal delivery systems for treatment of depression

Hanan Refai[1], Dina A. Osman[2], Maha K. A. Khalifa[2*] and Soha Elsalhy[1]

[1] Department of Pharmaceutics, College of Pharmaceutical Sciences and Drug Manufacturing, Misr University for Science and Technology (MUST), Al-Motameyez District, 6th October City, Giza, Egypt.
[2] Department of Pharmaceutics and Pharmaceutical Technology, Faculty of Pharmacy (Girls), Al-Azhar University, Nasr City, Egypt.
* Correspondence: Mahakhalifa.ahmed@hotmail.com , Mahakhalifa.pharmg@azhar.edu.eg ; Tel.: (+201008353149)

Article history: Received 2022-01-27 Revised 2022-02-20 Accepted 2022-03-04

Abstract: Trifluoperaizne (TFP) is an antipsychotic medication with limited oral bioavailability due to extensive first-pass metabolism; consequently, the goal of this project was to develop Leciplex nanoparticles to improve the bioavailability of TFP and to prolong its nasal residence time for treatment of the depression. Leciplex NPs were prepared using negatively charged phospholipid, cationic surfactant and biocompatible solvent and optimized using the 21 31 full factorial statistical design using various surfactants and different phospholipid to surfactant ratios. Design Expert® software was employed to select the optimum formula. The formulae were characterized regarding their particle size (PS), polydispersity index (PDI), zeta potential (ZP), entrapment efficiency percentages (EE %), amount of drug released after 6 hours (Q6h), transmission electron microscopy analysis, fourier transform infrared ray spectroscopy (FT-IR) and stability for six months. Optimized formula was contained dimethyldidodecylammonium bromide as surfactant and had a Phospholipon 90 G: surfactant ratio of 1:1. It showed a PS of 174.79 nm, a PDI of 0.241, a ZP of 38.21 mV, an EE% of 53.59 % and a Q6h of 65.58 %. The transmission electron microscopy analysis revealed that the nanoparticles were distinct, spherical in shape with a bright interior core and a black bilayer. The FT-IR studies suggested that there is no chemical interaction between TFP and polymers. Stability studies indicated that it was best to store nanoparticle formulations at 4°C. Thus, it can be inferred that the developed Leciplex could effectively be explored as a promising nasal delivery of TFP in the effective treatment of depression.

Keywords: Trifluoperazine hydrochloride; Leciplex; factorial design; nasal drug delivery.

1. INTRODUCTION

Traditionally, the nasal route has been used to provide medications for the treatment of local illnesses. However, in recent years, this route has garnered considerable attention as a simple and dependable way for systemic distribution of medications, particularly those that are inefficient by oral route due to gastrointestinal metabolism or first-pass impact and must be provided by injection. The nasal route of administration, as well as other suggested non-parenteral approaches, may fully meet the standards for systemic medicine use [1]. Due to the high permeability, high vasculature, low enzymatic environment of nasal cavity and avoidance of hepatic first pass metabolism are well suitable for systemic delivery of drug molecule via nose [2]. In spite of the nasal route's promise, various variables impede medication absorption intranasally. These obstacles include, the physical barrier of nasal epithelium by mucociliary clearance processes, enzymatic barrier of the nasal mucosa, and the nasal epithelium's limited permeability [3].

The utilization of medication delivery systems has stimulated the interest of researchers looking for ways to increase nasal drug absorption. Colloidal carrier technologies have shown significant efficacy in enhancing medication bioavailability via the nasal route [4].

The present study is aimed to manage depression using a nano formulations platform. Depression is a severe mental disorder marked by poor mood, low self-esteem, and a loss of interest or pleasure in ordinarily pleasurable activities [5]. It is characterized by a depressed mood, aversion to exercise, psychomotor agitation or retardation, sleeplessness or hypersomnia, exhaustion, intense feelings of guilt, worthlessness, difficulty concentrating, and suicidal thoughts. Major depression is a debilitating disorder that has a negative impact on a person's family, job or school life, sleep patterns, food habits, and overall health [6].

Trifluoperazine hydrochloride (TFP) is an antipsychotic drug often used to treat depression, agitation, anxiety, psychosis, and acute confessional condition [7]. This medicine has strong anticonvulsant characteristics and is commonly used in psychiatry to treat schizophrenia and other mental illnesses [8]. Because of its high first pass metabolism in the liver, it has a limited oral bioavailability [9]. TFP shows high water solubility and has an ionizable amine group with a pKa of 8.1 [10]. Because TFP is subject to first pass metabolism so its oral bioavailability is low, it is necessary to provide large doses often to keep the systemic drug concentration continuously above the desired therapeutic dosage [9].

An alternative approach to oral TFP administration is to incorporate the medication into submicroscopic nanoparticles and provide it via nasal route, concealing the drug molecule and delivering it to the systemic circulation in a controlled way, so avoiding first-pass metabolism.

Several attempts have been attempted to extend the nasal residence time by reducing the number of doses required, hence improving medicine absorption and promoting patient compliance [11]. Among of these attempts is the use of positively charged drug carriers such as which interact with the negatively charged sialic acid moieties present in the mucus membrane on nasal mucosa, resulting in improved nasal permeation [12]. Leciplex is a cationic nanocarrier that self-assembles from phospholipids designed for enhanced medication delivery of both hydrophilic and hydrophobic medicines [13]. It is a one-step manufacturing procedure that produces nanoscale vesicle systems with simple mixing, so it is easy to prepare [14]. The main components of Leciplex system are the negatively charged phospholipid (soy phosphatidylcholine), cationic surfactant (cetyltrimethylammonium bromide and dimethyldidodecylammonium bromide) and biocompatible solvent (transcutol) [14].

We aimed to develop an effective Leciplex nanoparticles (Leciplex NPs) using the 2^1 3^1 full factorial statistical design for intranasal delivery of TFP. All TFP-loaded Leciplex nanoparticle dispersions were evaluated for their particle size, zeta potential, polydispersity index, drug entrapment efficiency percentages and in vitro drug release.

2. METHODS

2.1. Materials

TFP was a gift from by Kahira Pharma & Chem. Ind. Co., Egypt. Highly purifief diehylene glycol monoethyl ether (Transcutol@ HP) was obtained from Gattefosse India Ltd., India. Phospholipon 90 G (PL-90G) was gifted from Lipoid GmbH, Germany. Cellulose membrane (12,000–14,000 molecular weight cutoff), Cetyltrimethylammonium bromide (CTAB) and Dimethyldidodecylammonium bromide (DDAB) were obtained from Sigma Aldrich Chemical Co., USA. Disodium hydrogen phosphate and potassium dihydrogen phosphate were obtained from El-Nasr Pharmaceutical Chemicals Co., Egypt.

2.2. Formulation of TFP-loaded Leciplex NPs

According to previously published procedures [15], Leciplexes were made in a one-step manufacturing process employing PL-90G and surface active agents (SAA) (CTAB or DDAB) in a molar ratio of 1:1 or 5:1 as stated in Table 1 [15]. TFP (50 mg) and PL-90G were dissolved in Transcutol® P (0.5 mL) by heating the mixture to 70 ºC in a constant temperature water bath (Superfit Ltd, Mumbai, India). A solution of CTAB or DDAB in water (9.5 ml, 70ºC) was immediately added to the TFP/PL-90G mixture with stirring (1200 rpm). The mixing process was continued until a uniform pale yellow dispersion of TFP-loaded Leciplexes NPs was obtained.

2.3. Statistic Optimization of TFP- loaded Leciplex NPs

Based on previous research [15], we chose PL-90G: SAA molar ratio with two levels and SAA type with three levels to be the independent variables, X1 and X2, respectively. Their effects on the responses of the developed formulation, namely particle size (PS) (Y1), and Polydispersity index

(PDI) (Y2), zeta potential (ZP) (Y3), entrapment efficiency percent (EE %) (Y4), and Q6h (Y5) were investigated using a 21.31 full factorial design (Table 1). Six formulations were prepared based on a multilevel categoric analysis (Design-Expert R software version 11 state-ease, Inc., Minneapolis, MN, USA), and their dependent variables were characterized, as shown in Table 1.

Table 1. Full factorial design ($2^1.3^1$) used for optimization of TFP loaded Leciplex NPs.

Factors (independent variables)	**Levels**
X1: PL-90G:SAA molar ratio	1:1, 5:1
X2: SAA type	No, CTAB, DDAB
Responses (dependent variables)	**Desirability constraints**
Y1: PS (nm)	Minimize
Y2: PDI	Minimize
Y3: ZP (mV)	Maximize (as absolute value)
Y4: EE%	Maximize
Y5: Q6h (%)	Maximize

2.4. Characterization of TFP- loaded Leciplex NPs

2.4.1. Particle size, polydispersity index and zeta potential

To measure the mean particle size and size distribution of freshly formed TFP-loaded Leciplex NPs dispersions, the Malvern Zetasizer 2000 (Malvern Instruments Ltd., Malvern, UK) was applied. The measurements were done after the samples had been diluted 100 times with double distilled water at room temperature [16]. Three measurements were made during a five minutes period, and the averages are reported.

2.4.2. Entrapment efficiency percentage (EE %)

Entrapment efficiency percentage (EE%) was calculated according to the method reported by Mohamed et al. [12]. The supernatant containing free TFP was obtained by subjecting samples to centrifugation using a cooling centrifuge (cooling ultracentrifuge 3–30 K, Sigma, Germany) at 20,000 rpm and 4 ºC , for 30 min. Using a micropipette, the clear supernatant was obtained. At 307 nm, the free drug concentration was evaluated spectrophotometrically (UV spectrophotometer; Shimadzu, Columbia, MD). The quantity of TFP entrapped in each formula was estimated according to this equation [17]:

EE%= (Total drug-Free drug in supernatant)/(Total drug)

2.4.3. In vitro release of TFP from TFP- loaded Leciplex NPs

TFP in vitro release was measured using the technique described by Morsi et al. [18]. The in vitro dissolution investigation was carried out using a modified USP-rotating basket dissolution apparatus (Hanson Elite 8, USA), glass cylinder tubes (10 cm long and 2.5 cm in diameter) attached to the shafts of the dissolution apparatus instead of baskets [12]. The other end of the glass tubes was securely wrapped in a cellulose membrane (12,000–14,000 molecular weight cutoff, Sigma Aldrich Chemical Co., USA) that had been soaked in phosphate buffer saline overnight (PBS, pH 6).

At 37±0.5 ºC and a spin speed of 50 rpm, the glass tubes containing 1ml of TFP-loaded Leciplex nanoparticle dispersions were submerged in 50 ml of PBS (pH 6). In this volume, the sink condition was maintained. At 0.25, 0.5, 1, 2, 3, 4, 5, and 6 h, samples were withdrawn and replaced with equal volumes of fresh media and tested spectrophotometrically at 307 nm [19]. The cumulative percent of TFP release was calculated. Experiments were performed in triplicate.

2.4.4. Kinetic studies of release

The in vitro release data were mathematically examined using zero order, first order, Higuchi model, and Korsmeyer–Peppas to study the mechanism of drug release.

2.5. Transmission Electron Microscopy (TEM)

The optimal nanoparticle was morphologically examined using TEM (JOEL JEM-1230, Japan). Place a drop of sample on a copper grid and allow to settling for 35 min. The excess liquid was then removed with absorbent paper. Prior to inspection with an acceleration voltage of 70 kV and magnification power of 150 KX 19, the sample was stained with a drop of an aqueous solution of phosphotungstic acid (2% w/v) for 3 min (2 % w/v) for 3 minutes [20].

2.6. Fourier Transform Infra-Red (FTIR) Spectroscopy

The possible interactions between TFP, PL-90G, DDAB, TFP/Leciplex physical combination, and freeze-dried TFP-loaded Leciplex NPs were investigated using FTIR spectroscopy. At room temperature, they were subjected to FT-IR analysis in the 400–4000 cm-1 range with a resolution of 4 cm-1 and a speed of 2 mm/s (Genesis II Mattson FT/IR spectrometer, Madison, WI). The band width was set to 50% of the peak height.

2.7. Stability Study on TFP- Loaded Leciplex Nps

The optimal TFP-loaded Leciplex NPs (L2) samples were stored at 4 ºC and 25 ºC for six months. Coalescence, settling, and colour change were visually assessed in the preserved samples. The PS, pH and EE% of the samples were determined and compared to fresh samples.

2.8. Statistical Analysis

Student's t-test was used to analyze data of two groups obtained in different experiments using GraphPad Instate 3 software and statistical significance was set at $p < 0.05$.

3. RESULTS

3.1. The Effect on Formulation Variables on Responses of

3.1.1. Particle size

Table (2) and Figure (1A) show the influence of the independent variables, PL-90G: SAA molar ratio (X1) and SAA type (X2) on particle size.

Table (2) shows that the particle sizes of TFP-loaded Leciplex NPs ranged from 114.54 nm to 588.20 nm (2). The acquired data were examined using polynomial analysis fitted with a quadratic model, yielding $p<0.0001$, indicating the model's significance. The predicted R^2 of 0.9170 was found to be reasonably close to the adjusted R^2 of 0.9390. Adequate precision is used to calculate the signal to noise ratio and a ratio larger than 4 is desired. In this situation, the ratio of 24.04 shows that the signal is appropriate, and the model might be utilized to navigate the design space. The relationship between PS and independent factors are depicted through the following polynomial equation:

PS (Y1) =325.01+76.56A-139.42B [1]-73.66B [2]

Where, A: PL-90G: SAA molar ratio; B: SAA type

The PL-90G: SAA molar ratio (X1) had statistically a significant ($p<0.0001$) positive impact on PS. Particle size was found to be greater in Leciplex formulae with a 5:1 molar ratio than in Leciplex formulations with a 1:1 molar ratio. The PS of nanoparticle also showed a significant ($p<0.0001$) positive impact considering the SAA type (X2). Firstly, presences of the SAA play a significant role in the PS of NPs. The nanodispersions contain only PL-90G (without CTAB/DDAB) showed particle size 460.13 nm and 524.73 nm for 1:1 and 5:1 PL-90G: SAA molar ratio, respectively. In contrast, NPs created with both CTAB and DDAB had smaller particle sizes when compared to nanoparticles prepared without CTAB/DDAB. These data revealed that the presence of cationic surfactant had a significant impact on the size of Leciplex particles. Secondly, the different types of SAA play also a role in particle size of NPs. The NPs containing CTAB showed lower particle size than to NPs containing DDAB.

3.1.2. Polydispersity index

Table (2) shows that the PDI of all TFP-loaded Leciplex NPs ranged from 0.206 to 0.683. The acquired data were examined using polynomial analysis fitted with a quadratic model, yielding $p<0.0001$, indicating the model's significance. The predicted R^2 of 0.8006 was found to be reasonably close to the adjusted R^2 of 0.8535. Adequate precision is used to calculate the signal to noise ratio and a ratio larger than 4 is desired. In this situation, a ratio of 12.23 shows that the signal is appropriate, and this model may be utilized to explore the design space. The relationship between PDI and independent factors are depicted through the following polynomial equation:

PDI (Y2) = 0.3796+0.0213A-0.1571B [1]-0.1172B [2]

Where, A: PL-90G: SAA molar ratio; B: SAA type

The ANOVA findings revealed that the SAA type (X2) had a significant ($P<0.0001$) negative impact on PDI as depicted in Table (2) and Figure (1B).

3.1.3. Zeta potential

The ZP of all TFP-loaded Leciplex NPs varied from -3.61 mV to +41.30 mV, as reported in Table (2). The acquired data were evaluated using polynomial analysis and a quadratic model, yielding $p<0.0001$, indicating the model's significance. The predicted R^2 of 0.9478 was found to be quite close to the adjusted R^2 of 0.9617. Adequate precision is used

to calculate the signal to noise ratio and a ratio larger than 4 is desired. In this case, a signal-to-noise ratio of 24.60 shows an appropriate signal, and this model may be utilized to explore the design space. The relationship between ZP and independent factors are depicted through the following polynomial equation:

ZP (Y3) = 24.38+1.92A+12.64B [1] +15.74B [2]
Where, A: PL-90G: SAA molar ratio; B: SAA type

Table (2) and Figure (1C) show the ZP values for TFP-loaded Leciplex NPs. The ANOVA findings revealed that SAA type (X2) had a significant ($P<0.0001$) positive impact on drug release. All DDAB/CTAB Leciplexes formulations showed positive surface charge (+32.77 to +41.3 mv) while both formulae (L3 and L6) which were formulated without cationic SAA showed negative ZP value (-4.36 and -3.60, respectively).

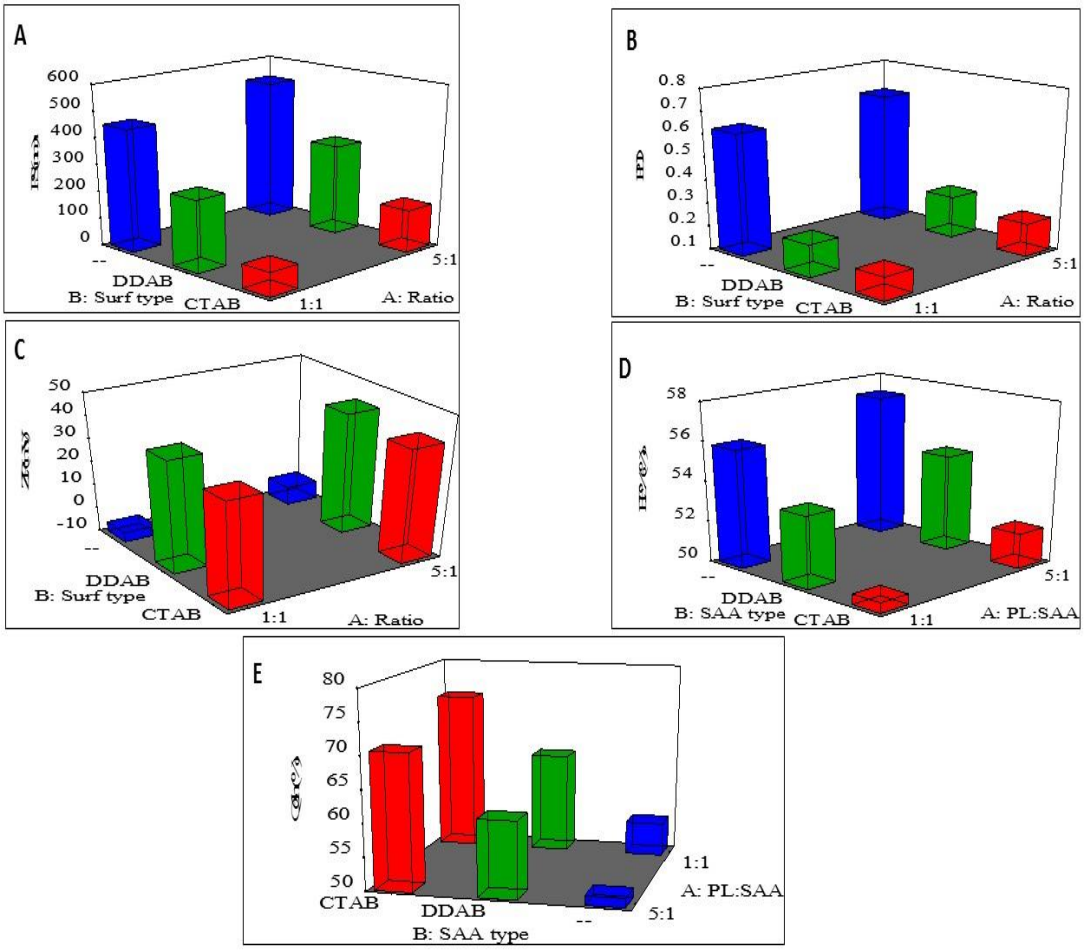

Figure 1. Response 3-D plots for the effect of PL-90G:SAA(X1), SAA type (X2) on (A) EE%, (B) PS, (C) PDI, (D) ZP, and (E) Q6h of TFP loaded Leciplex NPs.

Abbreviations: 3-D, three-dimensional; CTAB: cetyltrimethylammonium bromide; DDAB: dimethyldidodecylammonium bromide; EE%, entrapment efficiency percentage; NPs: nanoparticles; PS, particle size; PDI, polydispersity index; Q6h, amount of drug released after 6 hours; PL-90G: Phospholipon 90 G; SAA, surfactant;TFP: Trifuoperazine; ZP, zeta potential.

Table 2. Experimental runs, independent variables, and measured response of the 21.31 full factorial experimental design of TFP-loaded Leciplex.

Formula	X1	X2	Y1	Y2	Y3	Y4	Y5
	PL-90G: SAA molar ratio	SAA type	PS (nm)	PDI	ZP (mV)	EE% (%)	Q6h (%)
L1	1:1	CTAB	114.54±4.88	0.206±0.006	32.73±1.72	50.87±0.56	74.29±1.20
L2	1:1	DDAB	142.73±7.31	0.241±0.001	39.03±1.59	53.46±0.31	66.40±1.21
L3	1:1	--	488.07±67.4	0.625±0.143	-4.37±6.86	55.69±0.41	54.81±2.72
L4	5:1	CTAB	256.63±30.9	0.239±0.034	41.30±1.47	51.40±0.67	71.32±1.54
L5	5:1	DDAB	359.97±8.74	0.280±0.050	41.20±0.96	54.98±0.27	60.98±1.15
L6	5:1	--	588.20±54.8	0.683±0.151	-3.61±6.16	57.39±0.54	51.86±1.69

Note: Data represented as a mean ± SD (n=3).

3.1.4. Entrapment efficiency %

The EE% of all TFP-loaded Leciplex NPs ranged from 50.87 % to 57.39 %, as reported in Table (2). The acquired data were examined using polynomial analysis with a quadratic model, yielding $p<0.0001$, indicating the model's significance. It was discovered that the expected R^2 of 0.9342 was found to be quite close to the adjusted R^2 of 0.9516. Adequate precision is used to calculate the signal to noise ratio and a ratio larger than 4 is desired. In this situation, a ratio of 26.58 shows an adequate signal, and this model may be utilized to explore the design space. The relationship between EE% and independent factors are depicted through the following polynomial equation:

EE % (Y4) = 53.96+0.6253A-2.83B [1] +0.2531B [2]

Where, A: PL-90G: SAA molar ratio; B: SAA type

Table (2) and Figure (1D) show the influence of the independent variables PL-90G: SAA molar ratio (X1) and SAA type (X2) on the EE%. The ANOVA findings revealed that the PL-90G: SAA molar ratio (X1) had a significant positive impact on the EE% ($p=0.0002$). And also the SAA type (X2) affected on the EE% ($P<0.0001$). The nanodispersions with PL-90G only (without CTAB/DDAB) showed higher EE% 55.69 % and 57.39% for 1:1 and 5:1 PL: SAA molar ratio, respectively. By contrast, it was observed that NPs contain CTAB or DDAB were significantly ($P<0.0001$) high in EE% when compared with the nanoparticles prepared without CTAB/DDAB and the nanoparticles contain CTAB showed higher EE% than nanoparticles contain DDAB.

3.1.5. Amount of drug released after 6 hours

The Q6h of all TFP-loaded Leciplex NPs varied from 51.86 % to 74.72 %, as indicated in Table (2) and Figure (2). The received data were examined using polynomial analysis with a quadratic model, yielding $p<0.0001$, indicating the model's significance. It was discovered that the predicted R^2 of 0.9471 was found to be quite close to the adjusted R^2 of 0.9611. Adequate precision is used to calculate the signal to noise ratio and a ratio larger than 4 is desired. In this situation, a ratio of 29.26 indicates an adequate signal, and this model may be utilized to explore the design space. The relationship between Q6h and independent factors are depicted through the following polynomial equation:

Q6h (Y5) = 63.28-1.89A+9.53B [1] +0.4128B [2]

Where, A: PL-90G: SAA molar ratio; B: SAA type

All of the release profiles began with a burst release for the first two hours, followed by a constant steady release for the remaining six hours. Q6h values for TFP-loaded Leciplex nanoparticles were shown in Table (2) and Figure (1E). The ANOVA findings revealed that PL-90G: SAA molar ratio (X1) and SAA type (X2) had a significant negative impact on drug release. Regarding the PL-90G: SAA molar ratio (X1), it is clear that NPs created with a 1:1 PL-90G: SAA molar ratio have a greater TFP release rate at 6 hours from the formulations (L1, L2, L4, and L5), but NPs prepared with a 5:1

PL-90G: SAA molar ratio (L3 and L6) have a lower release rate.

Regarding SAA type (X2), it was found that the nanodispersions with PL-90G only (without CTAB/DDAB) showed lower percent of TFP released than the NPs contain CTAB/DDAB. And also, the NPs containing CTAB produced greater amount of TFP released relative to NPs containing DDAB.

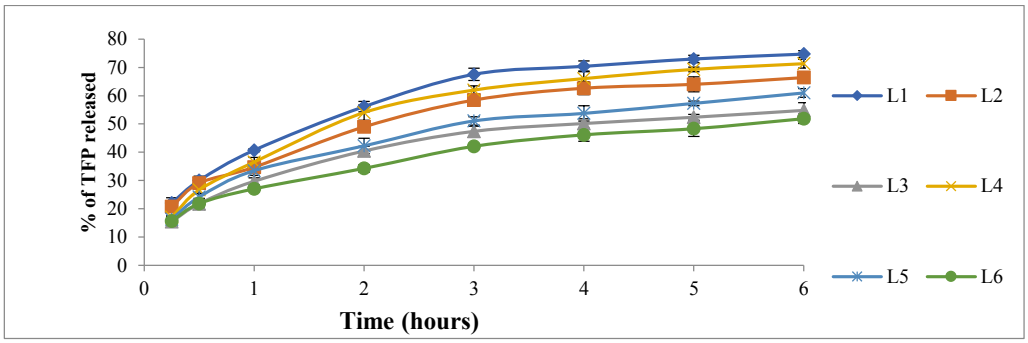

Figure 2. In vitro release profiles of TFP from nanoparticle nanodispersions in PBS (pH 6) at 37^{0}C (n=3).

3.2. Selection of the optimized formula

Based on the multilevel categoric model, an optimized formula containing DDAB as SAA and a PL-90G: SAA molar ratio of 1:1 was chosen. The PS was expected to be 174.79 nm, the PDI to be 0.241, the ZP to be 38.21 mV, the EE to be 53.59 %, and the Q6h to be 65.58 %. The optimized formula was evaluated and compared to the predicted values.

3.3. Kinetic studies of release

The in vitro release of all TFP-loaded Leciplex nanodispersion was studied using different kinetic models (zero-order, first-order, Higuchi, and Korsmeyer–Peppas equations) to determine the drug release mechanism (Table 3). In comparison to zero and first order, Korsmeyer–Peppas equation yielded the greatest r value for drug release.

Table 3. Kinetic studies of TFP-loaded Leciplex nanodispersion.

Formula Code	Correlation coefficient (R^2)				n	Release mechanism
	Zero order	First order	Higuchi model	Korsmeyer-peppas		
L1	0.877	0.967	0.985	**0.989**	0.321	Fickian
L2	0.855	0.958	0.969	**0.990**	0.368	Fickian
L3	0.845	0.937	0.945	**0.968**	0.401	Fickian
L4	0.926	0.978	0.987	**0.994**	0.346	Fickian
L5	0.931	0.977	0.987	**0.994**	0.415	Fickian
L6	0.859	0.922	0.951	**0.989**	0.321	Fickian

3.4. Transmission electron microscopy (TEM)

The morphology of fresh Leciplex nanoparticles (L2) was investigated using the TEM approach, as shown in Figure (3). The TEM micrograph of L2 NPs reveals a distinct, spherical vesicle with a bright interior core and a black bilayer.

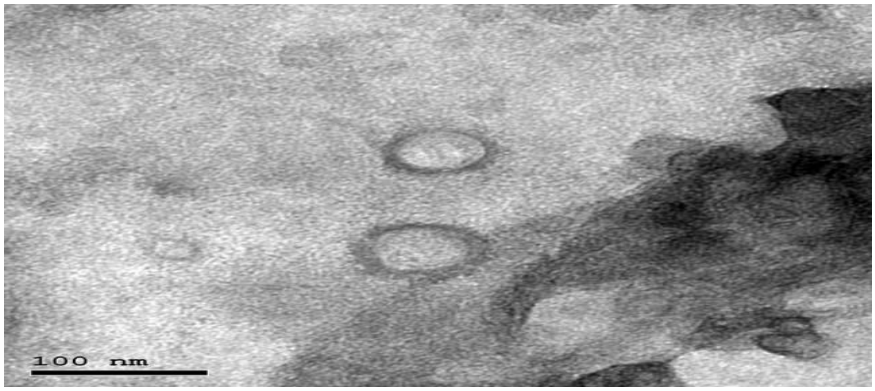

Figure 3. Transmission electron microscope (TEM) image of TFP loaded Leciplex NPs with optimum physicochemical characters (L2).

4.4. Fourier transform infra-red spectroscopy (FTIR)

Figure (4a) shows the spectrum of TFP with typical bands at 2958 cm^{-1} (N–H stretching). The bands at 1600 cm^{-1}, 1570 cm^{-1}, and 1492 cm^{-1} were caused by C=C aromatic. The bands at 823 cm^{-1} and 754 cm^{-1} were caused by aromatics that were 1,2,4 tri substituted and aromatics that were 1,2-substituted, respectively [21]. Figure (4b) shows the spectrum of PL-90G with bands at 2925 cm^{-1} and 2854 cm^{-1} (C–H stretching), 1737 cm^{-1} (C=O stretching band of ester), and 1240 cm-1 an ester (C–O stretching band of ester) [22]. Figure (4c) depicts a DDAB spectrum with major peaks including methylene bending vibrations from 1480 cm^{-1} to 1100 cm^{-1} and a typical C–N asymmetric stretching band from the ammonium group at 1485 cm^{-1} [23].

Figure (4d) depicts the FTIR spectrum of a physical mixture of TFP and PL-90G, which has peaks in nearly the same locations as its components. Figure (4c) shows the spectrum of Leciplexes NPs (L2), which displayed the normal TFP bands with no spectral changes.

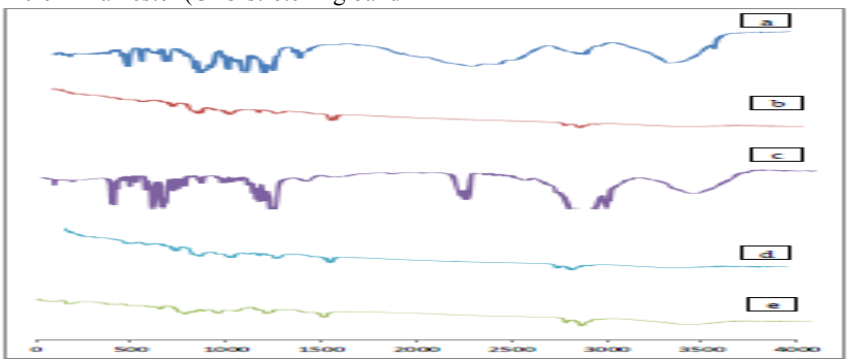

Figure 4. FT-IR spectra of a) trifluoperazine hydrochloride (TFP), b) Phospholipon® 90G (PL-90G), c) dimethyldidodecylammonium bromide (DDAB), d) their physical mixture and e) TFP loaded Leciplex formulation (L2).

4.5. Stability study on TFP loaded Leciplex nanodispersion

For 6 months, The NP formulations with the optimum characteristics (L2) were tested for visual examination, particle size, pH, and EE% at two different temperatures (25 ºC and 4 ºC). The outcomes are shown in Table (4). A minor agglomeration occurred after 6 months of storage; however, the particles persisted in the nano range. After 6 months of storage, it was also shown that the EE % was considerably ($p<0.05$) reduced to 46.67 % and 49.88 % at 25 ºC and 4 ºC, respectively.

Table 4. Effect of storage on the physical properties optimum nanodispersion (L2) during storage for 6 months.

Parameter	Time	25ºC	4ºC
PS	0	135.87±6.25	135.87±6.25
	3	394.70±23.83	152.83±10.79
	6	457.50±11.51	272.80±6.46
pH	0	6.1±0.00	6.1±0.00
	3	5.7±0.00	6.0±0.00
	6	5.5±0.00	5.8±0.00
EE%	0	53.46±0.31	53.46±0.31
	3	50.42±0.97	51.85±1.08
	6	46.67±1.23	49.88±1.17

4. DISCUSSION

The two-factor interaction model was chosen and it was noted that the predicted R^2 values were in a good agreement with the adjusted R^2. Adequate precision measures the signal to noise ratio to make sure that the model could be used to navigate the design space [24]. Adequate precision with a ratio greater than 4 is desirable which was observed in all responses.

It is obvious that raising the lipid concentration increases the particle size. Greater phospholipid content resulted in increased medium viscosity and more stiff solidified nanoparticles [25]. An excess of lipid might also explain the increased particle size by forming multilayers surrounding the particles and/or leaking into the aqueous phase, resulting in the production of extra vesicles or other aggregates [26]. This finding was in agreement with results observed by Hassan et al. who prepared carvedilol Leciplex for glaucoma treatment and also found that increase PL-90G: SAA molar ratio led to further increase in particle size of vesicles [15].

The addition of a cationic surfactant to Leciplex NPs resulted in a considerable reduction in particle size due to steric repulsion provided by surfactant molecules, which prevents or decreases vesicle aggregation [27]. It might also be attributed to a reduction in the aqueous-lipid interfacial tension, which results in the creation of smaller emulsion droplets [28]. The findings were in agreement with Date et al. who found that the Leciplex without CTAB/DDAB had higher particle size than Leciplex with CTAB/DDAB [13]. The NPs containing CTAB showed lower particle size than to NPs containing DDAB which might be because the mean particle size of double tail cationic surfactant (DDAB) Leciplex was larger than that of single tail cationic surfactant (CTAB) Leciplex [13]. It's probable that this is because DDAB with a double tail adsorbed better onto nanoparticles than CTAB with a single tail as well as the formation of the DDAB bilayer structure due to the van der Waals hydrophobic force of the DDAB double tails, which results in larger particle size [29].

The presences of the surfactants hold an inverse relationship with particle size. The nanodispersions with PL-90G only (without CTAB/DDAB) showed PDI 0.625 and 0.683 for 1:1 and 5:1 PL-90G: SAA molar ratio, respectively. By contrast, it was observed that NPs contain CTAB or DDAB had lower PDI values compared with the nanoparticles do not contain CTAB or DDAB. Surfactant provides aggregation stability by immediately covering the surface of freshly formed vesicles, preventing them from expanding into larger ones [27].

The positive charge of ZP of all DDAB/CTAB Leciplexes formulations caould be due to the surfactant's protonated amino group [30], indicating that the colloidal system is stable. The preference for positive charge in these formulations is to increase electrostatic interaction between cationic NPs and the negatively charged sialic acid residue of nasal mucosa. The findings were consistent with a study done by Hassan et al. who found that all formulae contain CTAB and DDAB had positive charge zeta potential [15]. The negative charge of ZP of the NPs which not contained cationic surfactants may be due to negatively charged phosphatidyl group of phospholipids. The findings were in agreement with Audu *et al.* who prepared solid lipid microparticles using Phospholipon 90G as a lipid matrix and the microparticles had a negative charge zeta potential [31].

Regarding to EE%, increase the phospholipid PL-90G: SAA molar ratio enhance the EE% by allowing more space for the medication to be incorporated. Increased lipid content expanded particle size and limited the chance of medications entering the external phase, which resulted for the increase in EE% [32]. Increase EE% in NPs which contained CTAB or DDAB might be attributable to CTAB and DDAB's capacity to increase incorporation of a drug into a phospholipid bilayer [33]. This finding was in agreement with Aggarwal *et al.* who encapsulated griseofulvin in deformable vesicles containing different surfactants as edge activators [34]. The higher EE% of CTAB NPs than DDAB NPs may be attributed to the difference in particle size between the nanoparticles. The increasing of particle size is accompanied by increasing in EE %. This is explained by a relative decrease in surface area as diameter increases, which increases the length of drug diffusional paths from the organic phase to the aqueous phase, reducing the chance of drug loss via diffusion towards the dispersion medium [35]. The findings were consistent with the findings of a previous study by Mohamed et al. who found that the entrapment efficiency increase with increasing the particle size [12].

Regarding to Q6h, increasing the PL-90G: SAA molar ratio led to lower release rate of TFP which may be due to increase the PS, resulting in a reduction in specific surface area and a slower release rate [12]. Increasing the lipid content resulted in higher medium viscosity and stiffer solidified nanoparticles. This may be slow drug diffusion into the dissolving media [25]. The results were in agreement with the study done by Tavakoli et al., who prepared sertaconazole-loaded lipid nanoparticles incorporated into thermosensitive in situ gel used for ocular administration [36]. And also, increasing the amount of TFP released from the CTAB NPs than DDAB NPs could be attributable to CTAB's higher hydrophilicity than DDAB and, as a result, increased solubility in medium when compared to DDAB. CTAB may solubilize TFP more effectively than DDAB over time, resulting in enhanced drug release [37]. This result was also due to the increase of the particle size led to decrease surface area/volume ratio which led to decrease buffer penetration and slow the release of the drug [38].

The optimized formula produced vesicles with a diameter of 169.17 nm, a PDI of 0.245, a ZP of 37.9 mV, an EE of 50.60 %, and a Q6h of 77.38 %. It had percent errors of 0.23 % for particle size and 0.021 % for EE %, respectively. This low magnitude of error implies that the multilevel categoric model is appropriate for optimizing Leciplex formulations and gives good prediction.

As a result of kinetic studies of release, diffusion is assumed to be the drug release mechanism. With n-values less than 0.5, they were also best fitted to the Korsmeyer–Peppas model, indicating the Fickian process.

The TEM micrograph of L2 NPs reveals a distinct, spherical vesicle with a bright interior core and a black bilayer. This finding was consistent with Salama et al. in the preparation of spironolactone loaded Leciplexes used for treatment of female acne [14]. Moreover, the nanoparticles appeared to be smaller than average particle size of the zetasizer. This might be due to hydrodynamic layers forming around the particles, leading the zetasizer to overestimate particle size [39].

The FT-IR study indicates a lack of chemical interaction between TFP and polymers and the stability study suggests that the encapsulated drug leaked from nanoparticles while being stored. This is almost certainly related to the drug's great hydrophilicity. It is worth noting that when the temperature was lower, system stability was enhanced.

4. CONCLUSION

In this study, cationic Leciplex was developed as a nasal delivery system for TFP. Six formulae were constructed using the $2^1.3^1$ full factorial design, and the optimal formula (L2) with small PS and low PDI, high ZP and EE% and TFP release was chosen. Based on the multilevel categoric model, the chosen optimized formula had a PL-90G: SAA molar ratio of 1:1 and DDAB as SAA. It had a PS of 174.79 nm, a PDI of 0.241, a ZP of 38.21 mV, an EE of 53.59 %, and a Q6h of 65.58 %. TFP loaded Leciplex might potentially be beneficial for a nasal delivery system for TFP, which could be used to treat depression.

Funding: This research received no external funding.

Acknowledgments: The authors would like to thank Kahira Pharmaceuticals and Chemical Industries Company for the supply of Trifluoperazine.

Conflicts of Interest: The authors declare no conflict of interest.

Author Contribution: All authors work in this paper in the practical and written work.

List of Abbreviations: 3-D, three-dimensional; CTAB: cetyltrimethylammonium bromide; DDAB: dimethyldidodecylammonium bromide; EE%, entrapment efficiency percentage; FT-IR, fourier transform infrared ray spectroscopy; NPs, nanoparticles; PS, particle size; PDI, polydispersity index; PL-90G: phospholipon 90 G; Q6h, amount of drug released after 6 hours; SAA, surfactant; TEM, transmission electron microscope; TFP: trifluoperazine; ZP, zeta potential.

REFERENCES

1. Krishnamoorthy R, Mitra AK. Prodrugs for nasal drug delivery. Adv Drug Del Rev. 1998;29(1-2):135-46.

2. Hinchcliffe M, Illum L. Intranasal insulin delivery and therapy. Adv Drug Del Rev. 1999;35(2-3):199-234.

3. Vyas TK, Shahiwala A, Marathe S, Misra A. Intranasal drug delivery for brain targeting. Curr Drug Del. 2005;2(2):165-75.

4. Mara Mainardes R, Cristina Cocenza Urban M, Oliveira Cinto P, Vinicius Chaud M, Cesar Evangelista R, Palmira Daflon Gremiao M. Liposomes and micro/nanoparticles as colloidal carriers for nasal drug delivery. Curr Drug Del. 2006;3(3):275-85.

5. Lenox RH, Frazer A, editors. Mechanism of action of antidepressants and mood stablizers. Neuropsychopharmacology: the fifth generation of progress Philadelphia: Lippincott Williams & Wilkins; 2002: Citeseer.

6. Kircanski K, Joormann J, Gotlib IH. Cognitive aspects of depression. Wiley Interdisciplinary Reviews: Cognitive Science. 2012;3(3):301-13.

7. Atta NF, Ahmed YM, BinSabt MH, Galal A. Hematite nanoparticles/ionic liquid crystal/graphene–based nanocomposite electrochemical sensor for sensitive determination of antipsychotic drug. J Electrochem Soc. 2016;163(14): B659-B66.

8. Vardanyan R, Hruby V. Synthesis of essential drugs: Elsevier; 2006.

9. Gahiwade HP, Patil MV, Tekade BW, Thakare VM, Patil V. Formulation and in-vitro evaluation of trifluoperazine hydrochloride bi-layer floating tablet. IJPBS. 2012;2(1):166-72.

10. Malheiros SVP, de Paula E, Meirelles NC. Contribution of trifluoperazine/lipid ratio and drug ionization to hemolysis. Biochim Biophys Acta. 1998;1373(2):332-40.

11. Li N, Zhuang C, Wang M, Sun X, Nie S, Pan W. Liposome coated with low molecular weight chitosan and its potential use in ocular drug delivery. Int J Pharm. 2009;379(1):131-8.

12. Mohamed S, Nasr M, Salama A, Refai H. Novel lipid–polymer hybrid nanoparticles incorporated in thermosensitive in situ gel for intranasal delivery of terbutaline sulphate. J Microencapsul. 2020;37(8):577-94.

13. Date AA, Srivastava D, Nagarsenker MS, Mulherkar R, Panicker L, Aswal V, et al. Lecithin-based novel cationic nanocarriers (LeciPlex) I: fabrication, characterization and evaluation. Nanomedicine. 2011;6(8):1309-25.

14. Salama A, Badran M, Elmowafy M, Soliman GM. Spironolactone-loaded leciplexes as potential topical delivery systems for female acne: In vitro appraisal and ex vivo skin permeability studies. Pharmaceutics. 2020;12(1):25.

15. Hassan DH, Abdelmonem R, Abdellatif MM. Formulation and characterization of carvedilol leciplex for glaucoma treatment: in-vitro, ex-vivo and in-vivo study. Pharmaceutics. 2018;10(4):197.

16. Abdelbary AA, Al-Mahallawi AM, Abdelrahim ME, Ali AM. Preparation, optimization, and in vitro simulated inhalation delivery of carvedilol nanoparticles loaded on a coarse carrier intended for pulmonary administration. International journal of nanomedicine. 2015; 10:6339.

17. Mohammadpourdounighi N, Behfar A, Ezabadi A, Zolfagharian H, Heydari M. Preparation of chitosan nanoparticles containing Naja naja oxiana snake venom. Nanomed Nanotechnol Biol Med. 2010;6(1):137-43.

18. Morsi N, Ghorab D, Refai H, Teba H. Nanodispersion-loaded mucoadhesive polymeric inserts for prolonged treatment of post-operative ocular inflammation. J Microencapsul. 2017;34(3):280-92.

19. Waleed AQ, Khammas ZA, Al-Ayash AS, Jasim F. An indirect atomic absorption spectrophotometric determination of trifluoperazine hydrochloride in pharmaceuticals. Arab J Sci Eng. 2011;36(4):553-63.

20. Khalifa MK, Salem HA, Shawky SM, Eassa HA, Elaidy AM. Enhancement of zaleplon oral bioavailability using optimized self-nano emulsifying drug delivery systems and its effect on sleep quality among a sample of psychiatric patients. Drug Deliv. 2019;26(1):1243-53.

21. De Lima LS, Araujo MDM, Quináia SP, Migliorine DW, Garcia JR. Adsorption modeling of Cr, Cd and Cu on activated carbon of different origins by using fractional factorial design. Chem Eng J. 2011;166(3):881-9.

22. Emami J, Mohiti H, Hamishehkar H, Varshosaz J. Formulation and optimization of solid lipid nanoparticle formulation for pulmonary delivery of budesonide using Taguchi and Box-Behnken design. Res Pharm Sci. 2015;10(1):17.

23. Schubert MA, Harms M, Müller-Goymann CC. Structural investigations on lipid nanoparticles containing high amounts of lecithin. Eur J Pharm Sci. 2006;27(2-3):226-36.

24. Yazhgur P, Noskov B, Liggieri L, Lin S-Y, Loglio G, Miller R, et al. Dynamic properties of mixed nanoparticle/surfactant adsorption layers. Soft Matter. 2013;9(12):3305-14.

25. Liu J, Gong T, Wang C, Zhong Z, Zhang Z. Solid lipid nanoparticles loaded with insulin by sodium cholate-phosphatidylcholine-based mixed micelles: preparation and characterization. Int J Pharm. 2007;340(1-2):153-62.

26. Ly M, Mekonnen TH. Cationic surfactant modified cellulose nanocrystals for corrosion protective nanocomposite surface coatings. J Ind Eng Chem. 2020;83:409-20.

27. Silva AM, Martins-Gomes C, Coutinho TE, Fangueiro JF, Sanchez-Lopez E, Pashirova TN, et al. Soft cationic nanoparticles for drug delivery: Production and cytotoxicity of solid lipid nanoparticles (SLNs). Appl Sci. 2019;9(20):4438.

28. Audu MM, Achile PA, Amaechi AA. Phospholipon 90G based SLMs loaded with ibuprofen: an oral anti-inflammatory and gastrointestinal sparing evaluation in rats. Pak J Zool. 2012;44(6).

29. Shah KA, Date AA, Joshi MD, Patravale VB. Solid lipid nanoparticles (SLN) of tretinoin: potential in topical delivery. Int J Pharm. 2007;345(1-2):163-71.

30. 30. Kumar GP, Rajeshwarrao P. Nonionic surfactant vesicular systems for effective drug delivery—an overview. Acta Pharm Sin B. 2011;1(4):208-19.

31. Aggarwal N, Goindi S. Preparation and evaluation of antifungal efficacy of griseofulvin loaded deformable membrane vesicles in optimized guinea pig model of Microsporum canis—Dermatophytosis. Int J Pharm. 2012;437(1-2):277-87.

32. Görner T, Gref R, Michenot D, Sommer F, Tran M, Dellacherie E. Lidocaine-loaded biodegradable nanospheres. I. Optimization of the drug incorporation into the polymer matrix. J Control Release. 1999;57(3):259-68.

33. Tavakoli N, Taymouri S, Saeidi A, Akbari V. Thermosensitive hydrogel containing sertaconazole loaded nanostructured lipid carriers for potential treatment of fungal keratitis. Pharm Dev Technol. 2019;24(7):891-901.

34. Dhawan VV, Joshi GV, Jain AS, Nikam YP, Gude RP, Mulherkar R, et al. Apoptosis induction and anti-cancer activity of LeciPlex formulations. Cell Oncol. 2014;37(5):339-51.

35. Mouez MA, Nasr M, Abdel-Mottaleb M, Geneidi AS, Mansour S. Composite chitosan-transfersomal vesicles for improved transnasal permeation and bioavailability of verapamil. Int J Biol Macromol. 2016;93:591-9.

36. Wu Y, Yang W, Wang C, Hu J, Fu S. Chitosan nanoparticles as a novel delivery

system for ammonium glycyrrhizinate. Int J Pharm. 2005;295(1-2):235-45.

37. Post A, Warren RJ, Zarembo JE. Trifluoperazine hydrochloride. Analytical profiles of drug substances. 9: Elsevier; 1981. p. 543-81.

38. Saoji SD, Raut NA, Dhore PW, Borkar CD, Popielarczyk M, Dave VS. Preparation and evaluation of phospholipid-based complex of standardized centella extract (SCE) for the enhanced delivery of phytoconstituents. AAPS J. 2016;18(1):102-14.

39. Mishra R, Mishra S, Upadhyay C, Prakash R. DDAB-Triggered, Size-Sorted, Instant Phase-Switching of Silver Nanoparticles. ChemistrySelect. 2017;2(10):3028-34.